THE PHASES DIFFERENTIAL ASTROMETRY DATA ARCHIVE. IV. THE TRIPLE STAR SYSTEMS 63 Gem A AND HR 2896

The Astronomical Journal, 140:1646–1656, 2010 December doi:10.1088/0004-6256/140/6/1646

THE PHASES DIFFERENTIAL ASTROMETRY DATA ARCHIVE. IV. THE TRIPLE STAR SYSTEMS 63 Gem A AND HR 2896

Matthew W. Muterspaugh[1,2], Francis C. Fekel[2], Benjamin F. Lane[3], William I. Hartkopf[4], S. R. Kulkarni[5], Maciej Konacki[6,7], Bernard F. Burke[8], M. M. Colavita[9], M. Shao[9], and M. Williamson[2]

[1] Department of Mathematics and Physics, College of Arts and Sciences, Tennessee State University, Boswell Science Hall, Nashville, TN 37209, USA; matthew1@coe.tsuniv.edu

[2] Tennessee State University, Center of Excellence in Information Systems, 3500 John A. Merritt Blvd., Box No. 9501, Nashville, TN 37209-1561, USA

[3] Draper Laboratory, 555 Technology Square, Cambridge, MA 02139-3563, USA; blane@draper.com

[4] U.S. Naval Observatory, 3450 Massachusetts Avenue, NW, Washington, DC 20392-5420, USA; wih@usno.navy.mil

[5] Division of Physics, Mathematics and Astronomy, 105-24, California Institute of Technology, Pasadena, CA 91125, USA

[6] Nicolaus Copernicus Astronomical Center, Polish Academy of Sciences, Rabianska 8, 87-100 Torun, Poland; maciej@ncac.torun.pl

[7] Astronomical Observatory, Adam Mickiewicz University, ul. Sloneczna 36, 60-286 Poznan, Poland

[8] MIT Kavli Institute for Astrophysics and Space Research, MIT Department of Physics, 70 Vassar Street, Cambridge, MA 02139, USA

[9] Jet Propulsion Laboratory, California Institute of Technology, 4800 Oak Grove Dr., Pasadena, CA 91109, USA

Received 2010 July 8; accepted 2010 September 19; published 2010 October 20

ABSTRACT

Differential astrometry measurements from the Palomar High-precision Astrometric Search for Exoplanet Systems (PHASES) are used to constrain the astrometric orbit of the previously known $\lesssim$2 day subsystem in the triple system 63 Gem A and have detected a previously unknown two-year Keplerian wobble superimposed on the visual orbit of the much longer period (213 years) binary system HR 2896. 63 Gem A was already known to be triple from spectroscopic work, and absorption lines from all three stars can be identified and their individual Doppler shifts measured; new velocities for all three components are presented to aid in constraining the orbit and measuring the stellar masses. In fact, 63 Gem itself is a sextuple system: the hierarchical triple (Aa1–Aa2)–Ab (in which Aa1 and Aa2 orbit each other with a rapid period just under 2 days, and Ab orbits these every two years), plus three distant common proper motion companions. The very small astrometric perturbation caused by the inner pair in 63 Gem A stretches the limits of current astrometric capabilities, but PHASES observations are able to constrain the orientation of the orbit. The two bright stars comprising the HR 2896 long-period (213 year) system have a combined spectral type of K0III and the newly detected object's mass estimate places it in the regime of being an M dwarf. The motion of the stars are slow enough that their spectral features are always blended, preventing Doppler studies. The PHASES measurements and radial velocities (when available) have been combined with lower precision single-aperture measurements covering a much longer time frame (from eyepiece measurements, speckle interferometry, and adaptive optics) to improve the characterization of the long-period orbits in both binaries. The visual orbits of the short- and long-period systems are presented for both systems and used to calculate two possible values of the mutual inclinations between inner and outer orbits of $152^\circ \pm 12^\circ$ or a less likely value of $31^\circ \pm 11^\circ$ for 63 Gem A and $10\overset{\circ}{.}2 \pm 2\overset{\circ}{.}4$ or $171\overset{\circ}{.}2 \pm 2\overset{\circ}{.}8$ for HR 2896. The first is not coplanar, whereas the second is either nearly coplanar or anti-coplanar.

Key words: astrometry – binaries: close – binaries: visual

1. INTRODUCTION

There are two major motivating factors for studying systems with three or more stars. The first is the determination of the fundamental properties of the stars themselves. Their masses, luminosities, and radii can be derived if high-resolution imaging and radial velocity (RV) orbits are combined. Through their physical association, one can assume that all stars in the system have identical ages, primordial elemental abundances, and similar histories. The only variations that can explain observed differences are the masses of the stars themselves. Binary stars have been important for establishing constraints on modeling stellar structure and evolution. These constraints become much more strict as the number of stars in a system grows—the science gained scales much faster than linear with the number of system components.

The second is the complex dynamics in systems with more than two components. The planets of our solar system are found in a flat disk. There is great interest in determining whether multiple star systems are equally coplanar because this tells about the formation environments of stars (Sterzik & Tokovinin 2002) and their subsequent evolutions (Fabrycky & Tremaine 2007). From the six triples and two quadruples studied so far, it is clear that the distribution is neither always coplanar nor is it consistent with randomly oriented subsystems.

To determine unambiguously a system's coplanarity, one must have both visual and RV orbital solutions for pairs of interest. The reason that mutual inclination measurements have been rare is because of the observational challenges these systems present. RV signals are largest for compact pairs of stars, whereas imaging prefers wider pairs. The "wide" pair must have large enough RV amplitude for a signal to be detected, thus its physical (and apparent) separation is as small as the two-component binaries that are already challenging for visual studies. The "narrow" pair is even smaller. This paper presents the geometries of two new triple star systems: 63 Gem A and HR 2896.

This paper is the fourth in a series, analyzing the final results of the Palomar High-precision Astrometric Search for Exoplanet Systems (PHASES) project after its completion in late 2008. The first paper describes the observing method, sources of measurement uncertainties, limits of observing precisions, derives empirical scaling rules to account for noise sources beyond those predicted by the standard reduction algorithms, and presents the full catalog of astrometric measurements from PHASES (Muterspaugh et al. 2010d). The second paper combines PHASES astrometry with astrometric measurements made by other methods as well as RV observations (when available) to determine orbital solutions to the binaries' Keplerian motions, determining physical properties such as component masses and system distance when possible (Muterspaugh et al. 2010b). The third paper presents limits on the existence of substellar tertiary companions, orbiting either the primary or secondary stars in those systems, that are found to be consistent with being simple binaries (Muterspaugh et al. 2010a). The current paper presents three-component orbital solutions to a known triple star system (63 Gem A = HD 58728) and a newly discovered triple system (HR 2896 = HD 60318). Finally, Paper V presents candidate substellar companions to PHASES binaries as detected by astrometry (Muterspaugh et al. 2010c).

63 Geminorum (HR 2846, HD 58728, ADS 6089, HIP 36238) is a hierarchical multiple system of six components. Its components have been studied in a variety of ways, including as spectroscopic, visual, common proper motion, and lunar occultation binaries. Component A, with composite spectral type F5 IV–V, is a subarcsecond hierarchical triple system (the components are Aa1, Aa2, and Ab), with additional faint common proper motion companions B, C, and D at distances of 43, 146, and 4 arcsec, respectively. The proper motions of A, B, and D are all similar and likely to be a true multiple system, but C is probably just an optical companion. This paper reports the three-dimensional orbits of the triple subsystem; components B, C, and D are not considered in the rest of the current study. The three components of subsystem A are organized as follows. A itself is split into two objects, designated Aa and Ab, which orbit each other with a period of ∼760 days. One of these, Aa, is itself a binary with components designated Aa1 and Aa2, which orbit each other with period ∼1.9 days. The wider pairing, Aa–Ab, was resolved with speckle interferometry (McAlister et al. 1983) and has been studied almost exclusively by speckle differential astrometry, with the occasional lunar occultation measurement. The short-period system has not been previously resolved, but has been monitored with RV. The high-precision (∼35 μas) differential astrometry technique developed by Lane & Muterspaugh (2004) has been used to measure the position vector between the Aa1–Aa2 center of light (COL) and the location of star Ab as part of PHASES (Muterspaugh et al. 2006). These measurements provide a detailed visual orbit of the Aa–Ab 760 day system, and also detect the 1.9 day COL wobble of the Aa1–Aa2 pair; these orbits are presented here. By combining astrometry and RV observations in a simultaneous fit, the mutual inclination between these pairs is measured, though with some ambiguity depending on whether Aa1 or Aa2 is more luminous at near-infrared *K*-band wavelengths (2.2 μm). Because Aa2 is less massive than Aa1, it is more likely that the solution favoring it being less luminous is correct.

HR 2896 (HD 60318, HIP 36896, WDS 07351 + 3058) was discovered to be a binary system with subarcsecond separation in 1842 by Struve (1878), though this result was not published until much later. The first published measurement of its binarity was reported by Maedler (1844). There is a faint C component at 82 arcsec, though it does not share a common proper motion and is probably not physical. Since the subarcsecond system was discovered, a number of visual observers and speckle interferometry teams have monitored the binary motion to map its very long period orbit. The latest program to monitor this pair, at yet higher astrometric precision, is PHASES, using long baseline interferometry and real-time phase-referencing techniques to measure binary separations with ∼35 μas repeatability. Model fitting the observed motion with a single Keplerian model provides unsatisfactory agreement with these higher precision observations, prompting a search for additional components to the system. A visual inspection of the residuals shows an obvious trend with a two year period.

Astrometric measurements were made at the Palomar Testbed Interferometer (PTI; Colavita et al. 1999). PTI was located on Palomar Mountain near San Diego, CA. It was developed by the Jet Propulsion Laboratory, California Institute of Technology for NASA, as a testbed for interferometric techniques applicable to the Keck Interferometer and other missions such as the *Space Interferometry Mission* (*SIM*). It operated in the *J* (1.2 μm), *H* (1.6 μm), and *K* (2.2 μm) bands, and combined starlight from two out of three available 40 cm apertures. The apertures formed a triangle with one 110 and two 87 m baselines. PHASES observations began in 2002 continued through 2008 November when PTI ceased routine operations.

2. ASTROMETRIC MEASUREMENTS

2.1. PHASES Measurements

Twenty-one differential astrometry measurements of 63 Gem A spanning 1495 days (nearly two orbits of the wide binary system) and 13 measurements of HR 2896 spanning 739 days were obtained with the procedure described by Lane & Muterspaugh (2004) and Paper I, with the use of the standard PHASES data reduction pipeline summarized in Paper I. No PHASES measurements are identified as significant outliers to the double Keplerian models, and all are used in orbit fitting.

Analysis of several PHASES binaries indicates that the formal measurement uncertainties evaluated by the standard data reduction pipeline underestimate the actual scatter in the measurements. As described by Paper I, a process for modifying the measurement uncertainties was found that best reproduces the observed scatter about Keplerian models for several binary targets. For measurements without the longitudinal dispersion compensator and/or automatic alignment system (as is applicable to all measurements of HR 2896), the solution is to increase the formal uncertainties along the error ellipse's major axis by a factor of 1.3 and then add 140 μas in quadrature, while for the minor axis the formal uncertainties are increased by a factor of 3.8 after which 35 μas is added in quadrature. When both the longitudinal dispersion compensator and automatic alignment system were operational (as was the case for about half of the 63 Gem A measurements), the same uncertainty corrections are applied except that the minor axis scaling factor is 1.0 instead of 3.8. The measurements and their associated formal and re-scaled measurement uncertainties are listed in Paper I. The average scaled measurement uncertainty is 61 μas in the minor axis and 499 μas in the major axis for 63 Gem A, and 40 μas and 228 μas for HR 2896, respectively.

2.2. Non-PHASES Astrometry Measurements

The wider pairing of 63 Gem A (Aa–Ab) was resolved for the first time with speckle interferometry by McAlister et al. (1983). This and other speckle interferometry measurements have been collected in the Washington Double Star Catalog (henceforth WDS; Mason et al. 2001, 2010, and see references to the original works therein) and are presented in Table 1.

Table 1
Non-PHASES Astrometric Measurements

HD Number	Date (year)	ρ (arcsec)	θ (deg)	σ_ρ (arcsec)	σ_θ (deg)	Weight	Outlier
58728	1980.1588	0.044	348.00	0.013	4.29	1.2	0
58728	1983.0476	0.114	346.60	0.005	1.64	8.2	0
58728	1983.9554	0.035	163.00	0.015	4.95	0.9	0
58728	1983.9583	0.036	171.50	0.015	4.70	1.0	0
58728	1984.8436	0.109	347.30	0.005	1.64	8.2	0
58728	1985.0000	0.104	347.20	0.005	1.75	7.2	0
58728	1985.1801	0.089	345.00	0.006	1.99	5.6	0
58728	1985.2050	0.071	354.50	0.046	14.86	0.1	0
58728	1986.8867	0.103	346.80	0.006	1.76	7.1	0
58728	1986.8893	0.104	347.10	0.005	1.75	7.2	0
58728	1987.2689	0.094	346.30	0.006	1.95	5.8	0
58728	1988.1648	0.047	181.20	0.014	4.48	1.1	0
58728	1988.2520	0.089	199.20	0.006	2.02	5.4	1
58728	1988.9098	0.106	350.00	0.018	5.62	0.7	0
58728	1989.1556	0.107	346.70	0.012	3.84	1.5	0
58728	1989.2295	0.102	346.70	0.006	1.76	7.1	0
58728	1993.2025	0.105	341.40	0.008	2.44	3.7	0
58728	1993.8396	0.061	350.60	0.008	2.71	3.0	0
58728	1994.8707	0.071	350.30	0.009	2.86	2.7	0
58728	1995.1490	0.094	347.00	0.010	3.10	2.3	0
58728	1995.3158	0.093	342.20	0.010	3.10	2.3	0
58728	1996.8636	0.087	340.70	0.011	3.41	1.9	0
58728	1997.0740	0.078	1.00	0.023	7.43	0.4	0
58728	1997.1259	0.094	348.10	0.008	2.59	3.3	0
58728	1997.8274	0.074	350.10	0.012	3.72	1.6	0
58728	1997.8274	0.072	352.30	0.012	3.84	1.5	0
58728	1999.1602	0.111	346.30	0.016	5.26	0.8	0
58728	2007.8230	0.114	347.80	0.008	2.48	3.6	0
58728	2007.8260	0.105	348.90	0.008	2.63	3.2	0
60318	1842.9500	0.500	331.20	0.101	3.56	0.7	0
60318	1843.2400	0.420	340.90	0.267	9.42	0.1	0
60318	1845.2700	0.470	332.60	0.109	3.85	0.6	0
60318	1846.3000	0.450	333.50	0.267	9.42	0.1	0
60318	1848.2900	0.440	329.00	0.101	3.56	0.7	0
60318	1851.3300	0.380	334.90	0.267	9.42	0.1	0
60318	1852.2500	0.460	331.40	0.134	4.71	0.4	0
60318	1854.2800	0.500	329.40	0.267	9.42	0.1	0
60318	1861.1899	0.620	328.80	0.120	4.21	0.5	0
60318	1869.5000	0.850	331.30	0.071	2.52	1.4	0
60318	1879.2500	0.720	334.50	0.101	3.56	0.7	0
60318	1879.7560	0.610	331.90	0.053	1.88	2.5	0
60318	1880.2000	0.900	331.70	0.154	5.44	0.3	0
60318	1883.4800	0.880	332.20	0.089	3.14	0.9	0
60318	1884.0400	0.750	332.80	0.040	1.42	4.4	0
60318	1885.0400	0.780	330.60	0.109	3.85	0.6	0
60318	1888.2380	0.710	334.10	0.051	1.78	2.8	0
60318	1889.9700	0.720	330.60	0.048	1.69	3.1	0
60318	1891.1479	0.690	329.70	0.085	2.98	1.0	0
60318	1893.1400	0.820	330.40	0.120	4.21	0.5	0
60318	1893.2500	0.500	329.90	0.154	5.44	0.3	0
60318	1894.2100	0.810	334.90	0.134	4.71	0.4	0
60318	1895.2500	0.730	332.40	0.120	4.21	0.5	0
60318	1896.0699	1.020	324.20	0.101	3.56	0.7	0
60318	1896.8700	1.000	329.00	0.081	2.84	1.1	0
60318	1896.8700	1.000	329.00	0.081	2.84	1.1	0
60318	1898.0900	0.820	328.70	0.065	2.29	1.7	0
60318	1898.2000	0.780	331.70	0.074	2.61	1.3	0
60318	1898.2500	0.720	331.50	0.101	3.56	0.7	0
60318	1898.2900	0.980	329.00	0.095	3.33	0.8	0
60318	1899.0601	0.730	333.40	0.089	3.14	0.9	0
60318	1899.0800	0.450	330.00	0.109	3.85	0.6	0
60318	1899.1500	0.610	334.50	0.101	3.56	0.7	0
60318	1900.0800	0.660	330.10	0.085	2.98	1.0	0
60318	1900.1899	0.710	329.00	0.120	4.21	0.5	0
60318	1901.1700	0.750	338.40	0.089	3.14	0.9	0

Table 1
(Continued)

HD Number	Date (year)	ρ (arcsec)	θ (deg)	σ_ρ (arcsec)	σ_θ (deg)	Weight	Outlier
60318	1901.2300	0.630	332.60	0.081	2.84	1.1	0
60318	1901.3199	0.610	324.90	0.134	4.71	0.4	0
60318	1902.2000	0.480	325.30	0.109	3.85	0.6	0
60318	1902.2100	0.640	325.60	0.095	3.33	0.8	0
60318	1902.2700	0.540	325.70	0.134	4.71	0.4	0
60318	1903.1600	0.550	330.10	0.077	2.72	1.2	0
60318	1903.2300	0.650	331.60	0.095	3.33	0.8	0
60318	1906.8400	0.790	331.30	0.085	2.98	1.0	0
60318	1908.2400	0.580	328.50	0.154	5.44	0.3	0
60318	1908.2500	0.840	331.30	0.267	9.42	0.1	0
60318	1909.1500	0.780	329.80	0.109	3.85	0.6	0
60318	1910.0500	1.020	332.20	0.101	3.56	0.7	0
60318	1910.0500	1.020	332.20	0.101	3.56	0.7	0
60318	1910.1390	0.630	322.60	0.085	2.98	1.0	0
60318	1910.1400	0.630	326.60	0.085	2.98	1.0	0
60318	1910.2000	0.780	328.90	0.120	4.21	0.5	0
60318	1910.2000	0.780	328.90	0.120	4.21	0.5	0
60318	1911.1700	0.730	332.20	0.077	2.72	1.2	0
60318	1911.9600	0.860	331.30	0.067	2.36	1.6	0
60318	1913.2300	0.780	331.40	0.081	2.84	1.1	0
60318	1914.1000	0.670	331.80	0.077	2.72	1.2	0
60318	1915.1899	0.530	331.10	0.089	3.14	0.9	0
60318	1917.3300	0.750	328.00	0.095	3.33	0.8	0
60318	1921.1400	0.860	330.90	0.052	1.85	2.6	0
60318	1923.2200	0.980	329.30	0.095	3.33	0.8	0
60318	1923.3101	0.650	330.60	0.120	4.21	0.5	0
60318	1923.3300	0.660	322.00	0.120	4.21	0.5	0
60318	1923.9570	0.805	332.70	0.089	3.14	0.9	0
60318	1925.0200	0.650	329.00	0.109	3.85	0.6	0
60318	1925.1400	0.780	329.10	0.109	3.85	0.6	0
60318	1925.1899	0.800	328.00	0.134	4.71	0.4	0
60318	1925.2000	0.840	328.80	0.109	3.85	0.6	0
60318	1927.1600	0.660	330.00	0.085	2.98	1.0	0
60318	1928.2100	0.770	327.70	0.047	1.67	3.2	0
60318	1930.4900	0.720	332.90	0.074	2.61	1.3	0
60318	1932.9200	0.730	329.00	0.069	2.43	1.5	0
60318	1933.1400	0.720	328.80	0.069	2.43	1.5	0
60318	1935.3700	0.700	327.60	0.056	1.96	2.3	0
60318	1936.1700	0.650	328.70	0.095	3.33	0.8	0
60318	1936.2200	0.600	332.80	0.120	4.21	0.5	0
60318	1937.0699	0.680	328.60	0.057	2.01	2.2	0
60318	1937.0800	0.860	328.30	0.067	2.36	1.6	0
60318	1937.8700	0.590	329.80	0.041	1.45	4.2	0
60318	1938.1100	0.550	328.90	0.109	3.85	0.6	0
60318	1939.2100	0.650	328.10	0.095	3.33	0.8	0
60318	1939.2300	0.640	328.30	0.067	2.36	1.6	0
60318	1939.2500	0.660	327.30	0.069	2.43	1.5	0
60318	1940.2100	0.680	327.80	0.134	4.71	0.4	0
60318	1941.2300	0.640	329.00	0.055	1.92	2.4	0
60318	1941.8101	0.750	330.00	0.101	3.56	0.7	0
60318	1943.3199	0.740	330.60	0.057	2.01	2.2	0
60318	1950.1400	0.570	328.00	0.109	3.85	0.6	0
60318	1950.1700	0.580	326.60	0.069	2.43	1.5	0
60318	1950.1801	0.530	327.60	0.065	2.29	1.7	0
60318	1950.1899	0.540	328.10	0.134	4.71	0.4	0
60318	1952.3199	0.530	327.60	0.067	2.36	1.6	0
60318	1953.2200	0.500	328.00	0.067	2.36	1.6	0
60318	1955.1700	0.520	327.80	0.069	2.43	1.5	0
60318	1955.2400	0.510	326.20	0.060	2.11	2.0	0
60318	1957.1801	0.450	326.20	0.067	2.36	1.6	0
60318	1958.4399	0.300	328.30	0.060	2.11	2.0	0
60318	1959.1500	0.360	324.40	0.058	2.06	2.1	0
60318	1959.2000	0.480	333.30	0.085	2.98	1.0	0
60318	1959.2200	0.380	328.70	0.095	3.33	0.8	0
60318	1959.6300	0.390	330.50	0.081	2.84	1.1	0

Table 1
(Continued)

HD Number	Date (year)	ρ (arcsec)	θ (deg)	σ_ρ (arcsec)	σ_θ (deg)	Weight	Outlier
60318	1959.9640	0.370	330.50	0.085	2.98	1.0	0
60318	1960.1300	0.500	333.40	0.067	2.36	1.6	0
60318	1960.1949	0.380	330.50	0.045	1.57	3.6	0
60318	1961.1700	0.340	323.50	0.085	2.98	1.0	0
60318	1961.1899	0.330	329.80	0.053	1.88	2.5	0
60318	1961.4000	0.330	326.70	0.074	2.61	1.3	0
60318	1962.0699	0.350	335.40	0.101	3.56	0.7	0
60318	1962.1700	0.330	329.00	0.049	1.72	3.0	0
60318	1962.9611	0.290	328.40	0.051	1.78	2.8	0
60318	1963.1010	0.310	328.30	0.154	5.44	0.3	0
60318	1963.1801	0.340	329.10	0.046	1.62	3.4	0
60318	1963.2200	0.370	326.90	0.134	4.71	0.4	0
60318	1964.2900	0.340	323.80	0.109	3.85	0.6	0
60318	1965.1340	0.330	329.00	0.052	1.85	2.6	0
60318	1965.1500	0.320	315.90	0.134	4.71	0.4	0
60318	1965.1899	0.260	333.40	0.061	2.16	1.9	0
60318	1965.6000	0.300	329.00	0.095	3.33	0.8	0
60318	1965.9900	0.340	331.00	0.039	1.39	4.6	0
60318	1966.1300	0.350	333.80	0.071	2.52	1.4	0
60318	1966.1429	0.240	324.80	0.065	2.29	1.7	0
60318	1966.1600	0.260	325.50	0.061	2.16	1.9	0
60318	1968.3149	0.220	308.60	0.267	9.42	0.1	0
60318	1968.9399	0.250	339.60	0.061	2.16	1.9	1
60318	1969.0760	0.180	325.90	0.089	3.14	0.9	0
60318	1969.2700	0.200	302.00	0.267	9.42	0.1	0
60318	1975.1200	0.100	258.00	0.267	9.42	0.1	0
60318	1976.8577	0.046	157.70	0.074	2.61	1.3	0
60318	1976.9233	0.052	157.10	0.065	2.29	1.7	0
60318	1977.0872	0.059	156.50	0.056	1.96	2.3	0
60318	1977.9146	0.081	150.60	0.081	2.84	1.1	0
60318	1977.9172	0.089	151.00	0.071	2.52	1.4	0
60318	1978.1492	0.088	154.00	0.037	1.29	5.3	0
60318	1979.7710	0.131	152.60	0.026	0.93	10.3	0
60318	1980.1536	0.141	150.90	0.025	0.87	11.7	0
60318	1980.7292	0.151	150.70	0.023	0.82	13.3	0
60318	1980.7828	0.147	149.30	0.025	0.90	11.0	0
60318	1980.8824	0.154	150.20	0.039	1.37	4.7	0
60318	1981.1500	0.160	145.50	0.154	5.44	0.3	0
60318	1981.9910	0.160	146.70	0.089	3.14	0.9	0
60318	1982.8521	0.188	151.40	0.109	3.85	0.6	0
60318	1983.0476	0.187	149.80	0.019	0.66	20.5	0
60318	1983.0601	0.210	149.10	0.109	3.85	0.6	0
60318	1983.2100	0.220	145.50	0.085	2.98	1.0	0
60318	1983.9341	0.261	157.00	0.085	2.98	1.0	0
60318	1983.9395	0.242	159.50	0.089	3.14	0.9	1
60318	1984.0526	0.198	150.10	0.018	0.62	23.2	0
60318	1984.0699	0.210	146.20	0.120	4.21	0.5	0
60318	1984.7870	0.204	150.30	0.101	3.56	0.7	0
60318	1985.1829	0.209	149.10	0.017	0.59	25.8	0
60318	1985.7450	0.225	143.90	0.095	3.33	0.8	0
60318	1985.8491	0.212	149.20	0.016	0.58	26.8	0
60318	1986.1899	0.220	144.90	0.069	2.43	1.5	0
60318	1986.2460	0.220	149.20	0.071	2.52	1.4	0
60318	1986.8894	0.212	148.20	0.016	0.58	26.8	0
60318	1987.1541	0.250	146.60	0.061	2.16	1.9	0
60318	1987.2690	0.214	148.70	0.016	0.57	27.4	0
60318	1988.9098	0.210	148.50	0.035	1.22	6.0	0
60318	1989.2140	0.260	142.90	0.060	2.11	2.0	0
60318	1989.2295	0.210	148.20	0.016	0.58	26.3	0
60318	1990.1010	0.240	143.10	0.058	2.06	2.1	0
60318	1990.2699	0.202	147.90	0.017	0.61	24.2	0
60318	1990.2754	0.201	148.30	0.017	0.61	23.9	0
60318	1991.0272	0.209	147.00	0.089	3.14	0.9	0
60318	1991.0353	0.219	148.00	0.081	2.84	1.1	0
60318	1991.2500	0.198	150.00	0.089	3.14	0.9	0
60318	1991.8943	0.198	147.70	0.018	0.62	23.2	0
60318	1992.2142	0.183	152.00	0.101	3.56	0.7	0
60318	1992.2202	0.180	152.00	0.101	3.56	0.7	0
60318	1992.2227	0.179	152.00	0.101	3.56	0.7	0
60318	1992.3068	0.191	147.80	0.018	0.64	21.4	0
60318	1993.1967	0.187	147.30	0.019	0.66	20.5	0
60318	1994.0925	0.176	147.40	0.030	1.05	8.0	0
60318	1995.1490	0.169	147.20	0.031	1.09	7.5	0
60318	1995.3131	0.167	147.30	0.031	1.10	7.4	0
60318	1995.9216	0.162	146.50	0.032	1.12	7.1	0
60318	1996.8638	0.150	146.00	0.035	1.23	5.9	0
60318	1997.1257	0.151	146.10	0.035	1.22	6.0	0
60318	1997.8275	0.143	145.30	0.036	1.28	5.4	0
60318	1997.8301	0.144	145.50	0.036	1.27	5.5	0
60318	1999.8182	0.135	147.60	0.074	2.61	1.3	0
60318	1999.8835	0.122	144.00	0.041	1.44	4.3	0
60318	2002.9993	0.090	148.00	0.065	2.29	1.7	0

Notes. Non-PHASES astrometric measurements from the WDS are listed with 1σ measurements uncertainties and weights. Column 1 is the HD Catalog number of the triple system, Column 2 is the decimal year of the observation, Columns 3 and 4 are the separation in arcseconds and position angle in degrees, respectively, Columns 5 and 6 are the 1σ uncertainties in the measured quantities from Columns 3 and 4, Column 7 is the weight assigned to the measurement, and Column 8 is 1 if the measurement is a $>3\sigma$ outlier and omitted from the fit, 0 otherwise.

A few lunar occultation measurements have also been conducted, though they are not included in the present analysis because they have little impact on the final orbital solution.

Differential astrometry of HR 2896 has a long history. Observations, spanning over 160 years, that used single-telescope techniques (including micrometry, speckle interferometry, and other interferometric techniques) have been cataloged in the WDS which includes 183 entries for HR 2896. These measurements are included in the present analysis to better constrain the much longer period A–B orbit.

Measurement uncertainties were evaluated with the algorithm for assigning weights, described by Hartkopf et al. (2001). Unit weight uncertainties were assigned separately for the separation and position angle measurements in such a way that the weighted root-mean-square scatter about a Keplerian model in each axis was unity. Measurements identified as more than a 3σ outlier in either separation or position angle were flagged as outliers, and the procedure was iterated until no outliers were found. One of the 29 measurements of 63 Gem A was found to be an outlier, and the unit weight uncertainties are 14.7 mas in separation and $4\overset{\circ}{.}70$ in position angle. The average uncertainties of the 28 measurements that were used are 11.4 mas and $3\overset{\circ}{.}7$, respectively, and the smallest values are 5.1 mas and $1\overset{\circ}{.}6$. Only two of the 183 measurements of HR 2896 were identified as outliers in this manner. The unit weight uncertainties are 84.6 mas in separation and $2\overset{\circ}{.}98$ in position angle. The average uncertainties of the 181 measurements being used are 86.4 mas and $3\overset{\circ}{.}04$; the smallest uncertainties are 16 mas and $0\overset{\circ}{.}57$. The measurements, their assigned uncertainties, and weights are listed in Table 1.

3. SPECTROSCOPIC MEASUREMENTS

3.1. 63 Gem A

Abt & Levy (1976) reported 20 RV measurements of component Aa1, and 17 of component Aa2 and determined the spectroscopic orbit of that subsystem. The scatter in the residuals resulting from a double-Keplerian model fit to these data suggests that the measurement uncertainties may be underestimated by a factor of 2.21 for component Aa1 and 3.83 for Aa2. The formal uncertainties reported in that work have been increased by these factors in order that this data set can be used in combined fits with others.

Twenty-six additional velocity measurements of all three components, and two of Aa1 and Ab, have been collected at Kitt Peak with the Coudé Feed Telescope and spectrograph, spanning eight years. Spectral features of all three components are present in these high-quality spectra. Tennessee State University (TSU)'s 2 m Automatic Spectroscopic Telescope (AST; Eaton & Williamson 2007) observed 63 Gem A 45 times over a 6.3 year period, spanning three orbits of the longer period Aa–Ab system. Spectral features of all three components are observed, and for each epoch the velocity of each star can be measured. All these spectroscopic measurements are used in the present analysis and are listed in Table 2 with the measurement uncertainties used during orbit fitting.

3.2. HR 2896

TSU's AST obtained spectra of HR 2896 on MJD 55267, 55272, 55276, 55286, 55295, 55304, 55321, and 55329. Only one set of absorption lines was observed, indicating blended lines and Doppler shifts too small to identify multiple components.

4. SEARCHING FOR THE SHORT SUBSYSTEM ORBITAL PERIODS

While the orbital periods of the second Keplerian perturbations were relatively obvious either from previous spectroscopic work (63 Gem A) or visual inspection of residuals to a single Keplerian model (HR 2896; see Figure 1), blind searches were conducted to ensure that aliased orbital periods were not being misidentified. An algorithm, based on that of Cumming et al. (1999, 2008), was modified for use on astrometric data for binary systems (described in Paper III) and used to conduct blind searches for tertiary companions in both systems.

The overall procedure is to create a periodogram of an F statistic comparing the goodness-of-fit χ^2 between a single Keplerian model and that for a double Keplerian model for a number of possible orbital periods for the second orbit. The orbital periods selected were chosen to be more than Nyquist sampled, to ensure complete coverage, as $P = 2fT/k$, where T is the span of PHASES observations, f is an oversampling factor, and k is a positive integer. Two searches were conducted for 63 Gem: first using only the PHASES measurements, and second using both the PHASES and non-PHASES astrometry to better constrain the wide binary motion during the search. Only the first of these searches was conducted for HR 2896, since the signal was very large. For both searches of 63 Gem A, $f = 2$ was chosen for computational efficiency, because the largest value of k was much larger than typical, corresponding to that for which the minimum period sampled was 1.1 days, to ensure inclusion of the expected $\lesssim 2$ day companion orbital period, and only positive integer values of k were evaluated. For the search of HR 2896, $f = 3$ was chosen, and the largest value of k corresponded to that for which the minimum orbital period examined was 6 days. In addition to the positive integer values of k, the period corresponding to $k = 1/2$ was evaluated to search for companions with orbits slightly longer than the PHASES span.

The orbital period for which the F statistic periodogram has its maximum value is the most likely orbital period of a companion object. To ensure the peak is a real object rather than a statistical fluctuation, 1000 synthetic data sets with identical cadence and measurement uncertainties as the actual data were created and evaluated in the same manner. The fraction of these having a maximum F statistic larger than that of the actual data provided an estimate of the false alarm probability (FAP) that the signal is not caused by an actual companion.

Because the 63 Gem Aa1–Aa2 subsystem has been well established by RV observations, it was not necessary that the astrometric data meet "detection" criteria to simply place constraints on an orbit. However, it is interesting to note that a wobble was detected in the PHASES data at a period near that of the RV signal, though not exactly overlapping. The peak in the 63 Gem A periodogram was at a period of 1.997 days in both the PHASES only and combined astrometry searches; for the former, the peak value was $z = 14.17$ with an FAP of 0.3%, whereas for the latter this improved to $z = 21.36$ with an FAP of 0.1%. However, the much higher signal-to-noise ratio RV signal was found to have an orbital period closer to 1.93 days; the PHASES measurements are consistent with this signal as well, though the search algorithm did not exactly reproduce this value. This is likely due to the low signal level of the astrometric perturbation and aliasing issues related to observing cadences. The periodograms of the 63 Gem data are presented in Figure 2.

For HR 2896, the 99% confidence level was at $z = 10.5$. With a maximum $z = 51.1$ at $P = 633$ days, none of the 1000 trials had z values exceeding that of the data; the FAP is estimated to be less than 0.1%. The 633 day orbital period was refined when the full double Keplerian model was fit to all the astrometric data. The periodograms of the HR 2896 data are presented in Figure 3.

5. ORBITAL MODELS

5.1. Orbit Fitting

Measurements were fit to models consisting of two Keplerian orbits superimposed on each other. One represented the motion of the wide system and the other that of the subsystem. The best-fit orbit parameters for the 63 Gem A and HR 2896 triple systems are listed in Table 3.

For 63 Gem A, with velocities of all three components, the total mass of Aa1–Aa2 can be determined by its motion in the wide Aa–Ab system and the part of its velocity from that. Coupled with the Aa1–Aa2 orbital period, this mass constrained the semimajor axis of the subsystem. When the Aa1 and Aa2 velocity signals from the subsystem motion were analyzed, this in turn constrained the inclination of the Aa1–Aa2 subsystem. Thus, just from a visual orbit of the outer system and radial velocities of all components, all parameters of the inner system are constrained except the longitude of the ascending node $\Omega_{\mathrm{Aa1-Aa2}}$. The high-precision PHASES astrometric measurements were necessary to constrain this one last parameter, crucial for understanding the overall system geometry. The Aa1–Aa2 COL motion is plotted in Figure 4 and the Aa1–Aa2 and Aa–Ab RV orbits are plotted in Figure 5.

For HR 2896, only astrometric measurements are available. From astrometry alone, it is impossible to tell which component contains the astrometric subsystem. In evaluating the orbital model parameters, it is assumed that the secondary is the

Table 2
Velocities of 63 Gem A

Day (HMJD)	RV_{Aa1} ($km\,s^{-1}$)	$\sigma_{RV,Aa1}$ ($km\,s^{-1}$)	RV_{Aa2} ($km\,s^{-1}$)	$\sigma_{RV,Aa2}$ ($km\,s^{-1}$)	RV_{Ab} ($km\,s^{-1}$)	$\sigma_{RV,Ab}$ ($km\,s^{-1}$)	Source
39157.337	106.8	3.5	...	...	...	...	Abt & Levy
39160.386	−0.7	2.7	...	...	...	...	Abt & Levy
39185.296	−53.0	2.9	...	...	...	...	Abt & Levy
39551.265	100.9	2.2	−102.1	10.7	...	...	Abt & Levy
39908.247	−22.9	2.7	93.5	10.3	...	...	Abt & Levy
40197.486	3.4	2.9	47.1	6.5	...	...	Abt & Levy
40198.485	59.9	4.0	−21.8	7.7	...	...	Abt & Levy
40280.221	90.3	1.8	−69.4	9.2	...	...	Abt & Levy
40281.221	−53.7	1.8	82.8	10.7	...	...	Abt & Levy
40518.545	−61.8	2.2	139.4	13.8	...	...	Abt & Levy
40519.507	114.7	2.2	−77.9	11.9	...	...	Abt & Levy
40526.497	−68.1	2.2	140.9	14.6	...	...	Abt & Levy
40549.428	−54.1	1.8	143.6	10.3	...	...	Abt & Levy
40550.508	125.9	1.3	−81.7	12.6	...	...	Abt & Levy
40872.520	−60.2	2.2	137.2	10.7	...	...	Abt & Levy
40873.475	118.2	2.4	−79.0	12.3	...	...	Abt & Levy
40874.486	−52.5	2.7	134.0	9.2	...	...	Abt & Levy
40901.503	−60.0	2.7	132.4	5.4	...	...	Abt & Levy
41044.143	−56.4	2.0	77.9	16.1	...	...	Abt & Levy
41045.176	96.8	2.0	−84.2	6.9	...	...	Abt & Levy
46076.850	97.7	1.0	−52.7	1.6	7.3	0.6	Kitt Peak
46130.777	126.9	1.0	−89.7	1.6	9.5	0.6	Kitt Peak
46389.026	−46.9	1.0	...	...	55.9	0.6	Kitt Peak
46389.859	95.0	1.0	−94.1	1.6	55.2	0.6	Kitt Peak
46390.944	−51.0	1.0	...	...	56.9	0.6	Kitt Peak
46530.690	115.2	1.0	−88.3	1.6	27.7	0.6	Kitt Peak
46531.714	−78.4	1.0	138.4	1.6	26.3	0.6	Kitt Peak
46533.725	−78.4	1.0	137.4	1.6	25.4	0.6	Kitt Peak
46534.686	119.8	1.0	−96.6	1.6	25.2	0.6	Kitt Peak
46722.041	125.5	1.0	−83.6	1.6	5.9	0.6	Kitt Peak
46814.903	131.2	1.0	−87.6	1.6	7.8	0.6	Kitt Peak
46816.851	129.0	1.0	−90.8	1.6	6.3	0.6	Kitt Peak
46868.805	108.6	1.0	−64.8	1.6	8.5	0.6	Kitt Peak
46869.737	−45.6	1.0	116.7	1.6	8.4	0.6	Kitt Peak
47097.014	116.3	1.0	−101.2	1.6	38.0	0.6	Kitt Peak
47098.850	106.9	1.0	−88.9	1.6	38.0	0.6	Kitt Peak
47152.056	−87.7	1.0	123.4	1.6	55.4	0.6	Kitt Peak
47153.030	105.6	1.0	−106.0	1.6	56.8	0.6	Kitt Peak
47247.736	111.4	1.0	−103.7	1.6	44.7	0.6	Kitt Peak
47248.769	−88.4	1.0	133.2	1.6	45.0	0.6	Kitt Peak
47308.632	−75.6	1.0	140.0	1.6	22.7	0.6	Kitt Peak
47310.635	−76.6	1.0	140.1	1.6	21.8	0.6	Kitt Peak
48345.670	122.9	1.0	−80.8	1.6	6.1	0.6	Kitt Peak
48346.661	−63.8	1.0	138.6	1.6	6.1	0.6	Kitt Peak
48506.023	123.8	1.0	−91.3	1.6	18.6	0.6	Kitt Peak
48770.648	108.8	1.0	−99.2	1.6	43.9	0.6	Kitt Peak
48774.628	115.5	1.0	−104.2	1.6	41.8	0.6	Kitt Peak
48912.880	−69.9	1.0	144.1	1.6	9.6	0.6	Kitt Peak
53022.316	113.3	0.635	−77.3	1.57	12.4	0.6	AST
53051.228	122.2	0.635	−89.2	1.57	15.1	0.6	AST
53298.534	110.4	0.635	−109.3	1.57	55.4	0.6	AST
53319.500	76.1	0.635	−62.7	1.57	47.7	0.6	AST
53329.506	113.3	0.635	−101.8	1.57	42.5	0.6	AST
53351.409	−49.3	0.635	100.3	1.57	33.3	0.6	AST
53357.399	−79.0	0.635	136.7	1.57	30.7	0.6	AST
53395.390	96.3	0.635	−63.8	1.57	20.0	0.6	AST
53442.303	−53.6	0.635	120.1	1.57	13.2	0.6	AST
53456.296	−39.0	0.635	104.8	1.57	12.3	0.6	AST
53486.192	107.6	0.635	−67.9	1.57	9.3	0.6	AST
53502.187	−46.4	0.635	114.3	1.57	9.0	0.6	AST
53693.554	−51.4	0.635	121.3	1.57	7.9	0.6	AST
53723.561	116.0	0.635	−77.2	1.57	8.8	0.6	AST
53742.445	−6.5	0.635	71.0	1.57	9.1	0.6	AST
53756.297	91.4	0.635	−49.7	1.57	11.0	0.6	AST
53769.265	−64.0	0.635	136.3	1.57	11.1	0.6	AST

Table 2
(Continued)

Day (HMJD)	RV_{Aa1} (km s^{-1})	$\sigma_{RV,Aa1}$ (km s^{-1})	RV_{Aa2} (km s^{-1})	$\sigma_{RV,Aa2}$ (km s^{-1})	RV_{Ab} (km s^{-1})	$\sigma_{RV,Ab}$ (km s^{-1})	Source
53786.375	−62.7	0.635	133.8	1.57	12.5	0.6	AST
53799.329	98.5	0.635	−59.4	1.57	14.3	0.6	AST
53818.278	117.1	0.635	−84.8	1.57	15.5	0.6	AST
53849.229	118.1	0.635	−89.6	1.57	19.5	0.6	AST
53863.178	77.6	0.635	−43.6	1.57	21.4	0.6	AST
53877.160	−57.3	0.635	115.2	1.57	23.3	0.6	AST
54100.527	115.9	0.635	−102.2	1.57	37.8	0.6	AST
54128.395	−57.6	0.635	115.0	1.57	27.1	0.6	AST
54845.366	−52.6	0.635	95.3	1.57	43.7	0.6	AST
54847.341	−62.2	0.635	107.3	1.57	43.7	0.6	AST
54879.190	88.2	0.635	−61.6	1.57	29.1	0.6	AST
54905.329	−53.9	0.635	116.2	1.57	22.5	0.6	AST
54920.186	114.3	0.635	−81.7	1.57	19.2	0.6	AST
54943.220	126.3	0.635	−95.2	1.57	15.5	0.6	AST
54952.182	−42.1	0.635	106.3	1.57	15.1	0.6	AST
54965.167	−34.0	0.635	98.3	1.57	12.2	0.6	AST
55105.456	123.4	0.635	−81.7	1.57	5.6	0.6	AST
55119.408	85.4	0.635	−41.9	1.57	6.7	0.6	AST
55146.261	125.3	0.635	−83.7	1.57	5.7	0.6	AST
55157.462	86.6	0.635	−41.6	1.57	6.1	0.6	AST
55199.314	−72.7	0.635	148.7	1.57	7.7	0.6	AST
55278.296	−40.0	0.635	106.7	1.57	11.7	0.6	AST
55283.231	116.2	0.635	−77.3	1.57	10.9	0.6	AST
55287.196	126.2	0.635	−92.3	1.57	11.4	0.6	AST
55292.252	−58.9	0.635	129.7	1.57	11.7	0.6	AST
55297.219	82.9	0.635	−40.3	1.57	12.3	0.6	AST
55311.236	−58.6	0.635	126.4	1.57	13.0	0.6	AST
55321.155	−70.4	0.635	141.7	1.57	14.5	0.6	AST

Note. Radial velocity measurements of 63 Gem A.

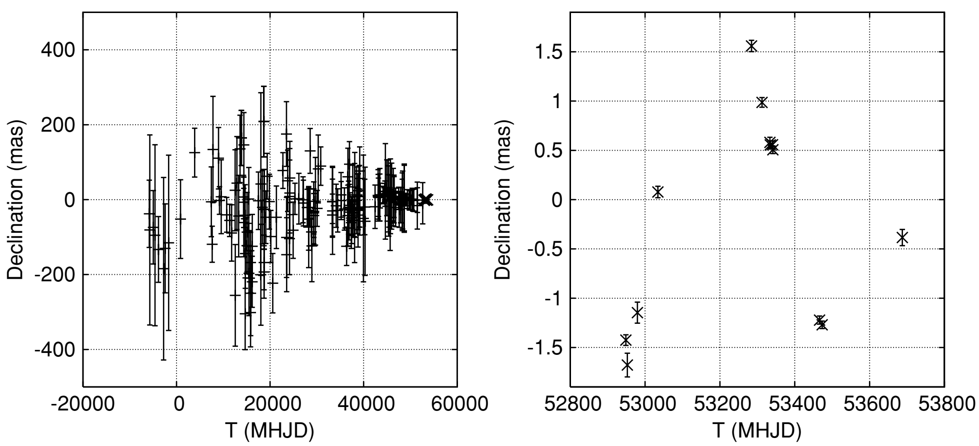

Figure 1. Residuals to a single Keplerian fit to the HR 2896 astrometry measurements, in the declination axis. Left: both PHASES (X symbols)and non-PHASES (+ symbols) measurements are shown. Right: for clarity, only PHASES measurements are shown. The presence of a long-period tertiary companion is obvious in the PHASES measurements. A refined search confirmed the signal is Keplerian with a period of ∼700 days.

subsystem, though this is an arbitrary selection. The COL motion of the HR 2896 subsystem is plotted in Figure 6.

Without a second Keplerian, HR 2896 fit a single Keplerian model with $\chi^2 = 8037.7$ and 381 degrees of freedom, for a reduced $\chi_r^2 = 21.1$. The double Keplerian model represented the data much better: $\chi^2 = 432.6$ with 374 degrees of freedom and $\chi_r^2 = 1.16$.

The orbital period of the subsystem in HR 2896 is almost exactly two years. While this can be a source of some concern about systematic effects, the large signal, its presence in two dimensions, and the fact that it does not appear in any of the other PHASES binaries lessens this concern. Coincidentally, the period of the outer pair of 63 Gem A (760 days) is nearly equal to that of the inner pair in HR 2896 (730 days); this demonstrates the great variety of configurations of hierarchical triple star systems.

5.2. Derived Quantities

For HR 2896, the *Hipparcos* parallax of 10.78 ± 1.16 mas was used to set an overall physical scale size for the system; this uncertainty was added in quadrature in the standard manner for first-order error propagation when calculating other derived quantities' uncertainties. From the binary (wide system) orbital period, semimajor axis, and the parallax, the total system mass

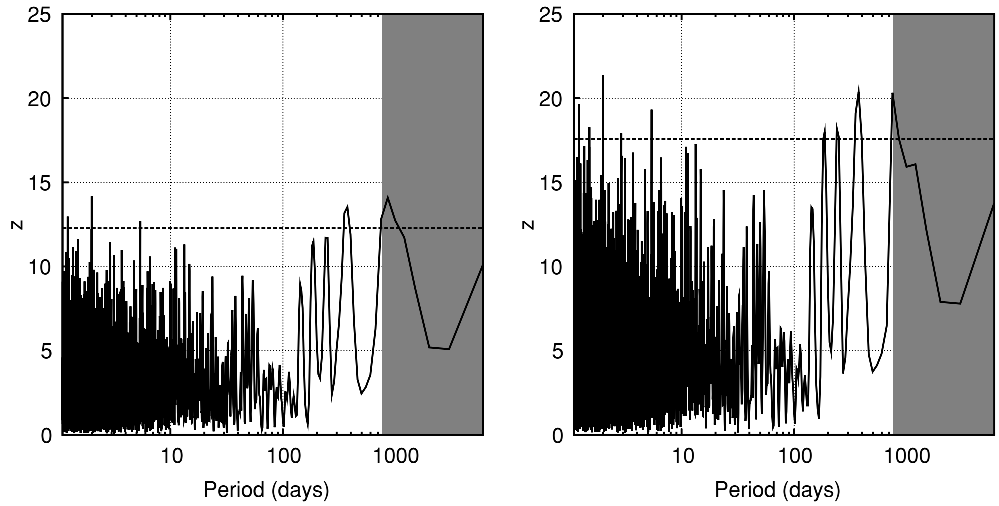

Figure 2. Periodograms of the F statistic (discussed in the text and written here as z) for 63 Gem A. The larger the value of z, the more likely the data are to represent the presence of a third component at the given period. Orbital periods longer than 760 days are unphysical, as this is the orbital period of the wider system itself; these regions are shaded in the plots. The left figure is for analysis only using the PHASES data, while the right is for combined analysis of PHASES and non-PHASES astrometric measurements. For 63 Gem A the 99% confidence level is at $z = 12.3$ for the PHASES-only analysis, and $z = 17.6$ for the combined analysis, as indicated by horizontal lines.

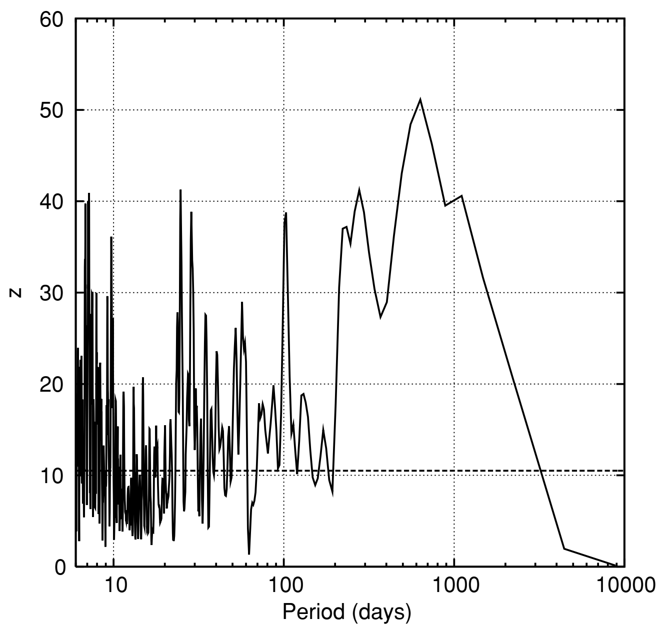

Figure 3. Periodogram of the F statistic (discussed in the text and written here as z) for HR 2896. The larger the value of z, the more likely the data are to represent the presence of a third component at the given period. For HR 2896 the 99% confidence level is at $z = 10.5$, indicated by a horizontal line.

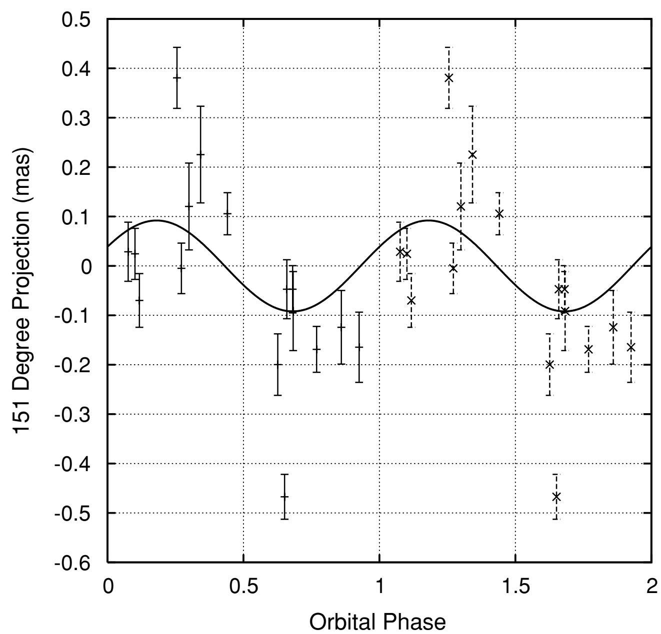

Figure 4. Center-of-light orbit of the ~1.9 day 63 Gem Aa1–Aa2 subsystem, along an axis at angle 151°, measured from increasing differential right ascension through increasing differential declination; it was along this axis that the PHASES measurements were typically most sensitive. For clarity, only measurements with uncertainties along this axis of $<100\,\mu$as are shown, and the measurements have been phase-wrapped about the 1.9 day orbital period and double-plotted to cover two cycles.

is found to be $3.00 \pm 0.98\, M_{\odot}$. Without a mass ratio, it was assumed that this mass is divided evenly between components (that is, the 730 day subsystem has total mass $1.50\, M_{\odot}$, equal to that of the other component). While this is very inexact, it nonetheless allows an estimate of the mass and nature of the unseen perturber.

Assuming a total mass of $1.50\, M_{\odot}$, the 730 day orbital period, COL semimajor axis (taken to be the true deflection of the more luminous component of the subsystem, an approximation justified when the perturber's mass was determined), and the parallax, a mass of $0.202\, M_{\odot}$ was derived. The approximation that the luminosity of the perturber can be ignored was justified since such a low-mass star would be far fainter than a K giant. Furthermore, even if the subsystem's total mass were assigned to be $3.98\, M_{\odot}$ (the 1σ upper bound of the total three body mass), the mass of the perturber would be only $0.39\, M_{\odot}$, still in the range of M dwarfs and still far less luminous than a K giant.

HR 2896 is likely to be in a stable configuration. Based on a large sample of gravitational simulations of test masses in binary systems, Holman & Wiegert (1999) formulated an empirical criteria for whether a tertiary companion can be stable long term. Their formula indicates that objects with periods as long as 2100 days would be stable in HR 2896.

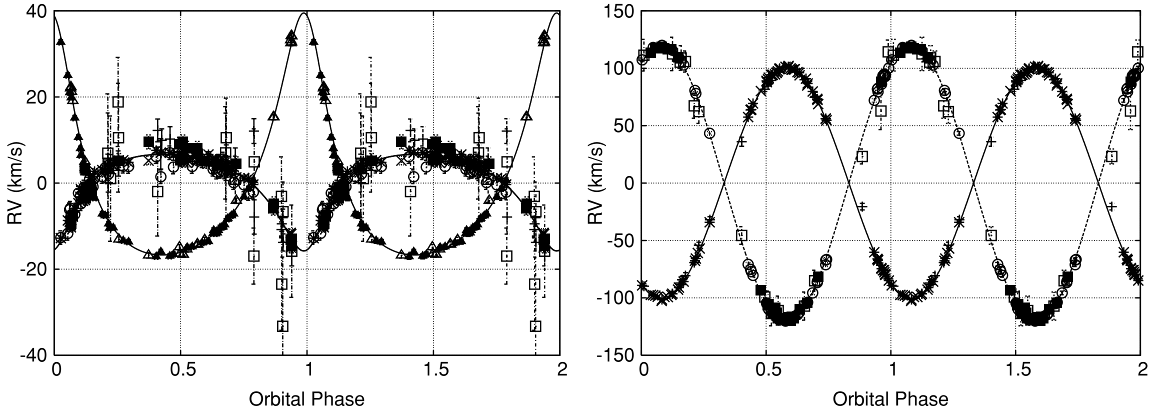

Figure 5. Left: radial velocity orbit of 63 Gem Aa-Ab, the outer pair. For clarity, the system velocity offset and Aa1–Aa2 signals have been removed, and the data were phase-wrapped about the 760 day orbital period. Two cycles of the orbit are shown for continuity (the measurements are double-plotted). Right: radial velocity orbit of the 63 Gem Aa1–Aa2 subsystem. Again the system velocity offset and Aa–Ab signal have been removed, and the data were phase-wrapped about the 1.9 day orbital period and double-plotted. Measurements by Abt & Levy (1976) are marked by + and unfilled square symbols for components Aa1 and Aa2, respectively. Measurements from Kitt Peak are marked by ×, filled square, and open triangle symbols for components Aa1, Aa2, and Ab, respectively. Measurements from the AST are marked by asterisks, open circles, and filled triangle symbols for components Aa1, Aa2, and Ab, respectively.

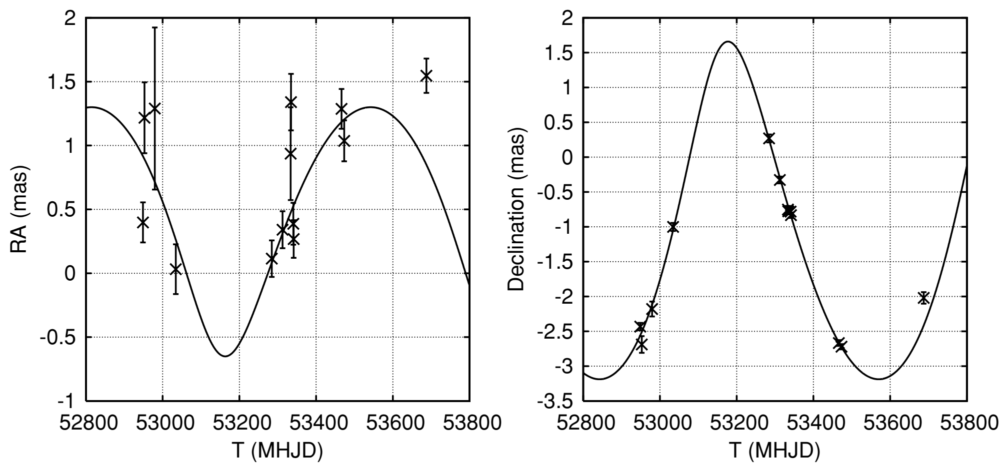

Figure 6. Motion of the center-of-light of the 730 day subsystem in HR 2896. Left: the motion in the right ascension axis, which was typically lower precision for the single baseline interferometric measurements (which were most often taken with the nearly north–south baseline at PTI). Right: the motion in the declination axis.

From the total subsystem mass approximation of $1.50 \pm 0.49\, M_\odot$ and 730 day orbital period, the full semimajor axis of the subsystem is 19.5 ± 3.0 mas. This is half the resolution of the *Hubble Space Telescope* and most infrared adaptive optics systems, but is easily in range of long baseline interferometry systems if high contrast ratios are possible. The high-precision closure phases being obtained by the MIRC beam combiner at CHARA (Monnier et al. 2004; ten Brummelaar et al. 2005) might enable imaging of the third component. Since it is likely the tertiary is a very red star, infrared imaging is likely to be advantageous for reducing the contrast requirements. From the parallax, it is found that the wider binary has a semimajor axis of 51.5 ± 5.6 AU and the subsystem has a semimajor axis of 1.81 ± 0.20 AU. Thus, the high eccentricity of the wide pair (0.6756 ± 0.0051) brings the outer star to within a factor of 10 of the size of the subsystem itself.

It is impossible to discern between two possible values of the mutual inclination of the two orbits from astrometry alone, because one must identify which node is ascending. From astrometry, two orbital solutions are possible, separated by changing both Ω and ω by 180° in either (or both) orbits. The mutual inclination of the orbits is given by

$$\cos\Phi = \cos i_1 \cos i_2 + \sin i_1 \sin i_2 \cos(\Omega_1 - \Omega_2), \qquad (1)$$

where i_1 and i_2 are the orbital inclinations and Ω_1 and Ω_2 are the longitudes of the ascending nodes. For HR 2896, the two possible values are $10\overset{\circ}{.}2 \pm 2\overset{\circ}{.}4$ or $171°2 \pm 2°8$. These values are very close to being either coplanar or anti-coplanar; in either case, this is relatively rare for a triple star system.

Even when a COL astrometric orbit and radial velocities are available for the narrow pair, there can be a degeneracy between which node is ascending and the luminosity ratio. Having found one possible luminosity ratio $L_{\mathrm{Aa2}}/L_{\mathrm{Aa1}} = L_1$, it can be shown that the other possible solution, corresponding to varying the ascending node by 180°, is given by

$$L_2 = \frac{2R + RL_1 - L_1}{1 + 2L_1 - R}, \qquad (2)$$

where R is the mass ratio $M_{\mathrm{Aa2}}/M_{\mathrm{Aa1}}$.

For 63 Gem A it is possible to lift the degeneracy, because the solution for which $L_{\mathrm{Aa2}}/L_{\mathrm{Aa1}} = 1.47 > 1$ is inconsistent with the spectral line strengths. Thus, the mutual inclination was determined without ambiguity to be $152° \pm 12°$. This is near the range $39\overset{\circ}{.}2$–$140\overset{\circ}{.}8$, where Kozai oscillations between inner pair orbital inclination and eccentricity are driven (Kozai 1962). Furthermore, the large mutual inclination again shows that star systems tend not to be coplanar, unlike the

Table 3
Orbit Models for 63 Gem A and HR 2896

Parameter	63 Gem A		HR 2896	
	Value	Uncertainty	Value	Uncertainty
$P_{\rm Wide}$ (days)	760.083	±0.081	77931	±1097
$T_{\rm Wide}$ (MHJD)	54038.6	±1.3	44117	±93
$e_{\rm Wide}$	0.4150	±0.0014	0.6756	±0.0051
$a_{\rm Wide}$ (arcsec)	...	...	0.5554	±0.0075
$i_{\rm Wide}$ (deg)	92.31	±0.12	91.788	±0.042
$\omega_{\rm Wide}$ (deg)	192.15	±0.59	137.5	±1.1
$\Omega_{\rm Wide}$ (deg)	346.930	±0.060	329.89	±0.14
$P_{\rm subsystem}$ (days)	1.93267835	$\pm 4.2 \times 10^{-6}$	727.9	±8.6
$T_{\rm subsystem}$ (MHJD)	54051.14	±0.46	53876	±19
$e_{\rm subsystem}$	0.0012	±0.0019	0.339	±0.074
$a_{{\rm COL},\,Ba-Bb}$ (arcsec)	...	...	0.00263	±0.00017
$i_{\rm subsystem}$ (deg)	69.9	±1.2	86.2	±1.6
$\omega_{\rm subsystem}$ (deg)	151	±86	338.6	±6.6
$\Omega_{\rm subsystem,1}$ (deg)	145	±16	158.5	±2.8
$\Omega_{\rm subsystem,2}$ (deg)	325	±16	338.5	±2.8
$V_{\rm 0,Abt\,\&\,Levy}$ (km s^{-1})	24.57	±0.81	...	...
$V_{\rm 0,Kitt\,Peak}$ (km s^{-1})	22.70	±0.16	...	...
$V_{\rm 0,AST}$ (km s^{-1})	22.56	±0.11	...	...
$M_{\rm Aa1+Aa2}$ ($M_\odot$)	2.583	±0.059	...	...
$M_{\rm Aa2}/M_{\rm Aa1}$	0.8422	±0.0029	...	...
$L_{\rm Aa2}/L_{\rm Aa1}$ (Option 1)	0.469	±0.099	...	...
$L_{\rm Aa2}/L_{\rm Aa1}$ (Option 2)	1.47	±0.28	...	...
M_{Ab} ($M_\odot$)	1.030	±0.038	...	...
d (parsec)	33.09	±0.28	...	...
χ^2 and DOF	926.1	332	432.6	374
Φ_1 (deg)	152	±12	10.2	±2.4
Φ_2 (deg)	31	±11	171.2	±2.8
$M_{\rm Aa1}$ ($M_\odot$)	1.402	±0.032	...	...
$M_{\rm Aa2}$ ($M_\odot$)	1.181	±0.027	...	...
M_{Ba} ($M_\odot$)	...	...	1.3	...
M_{Bb} ($M_\odot$)	...	...	0.2	...
$a_{\rm Wide}$ (arcsec)	0.07558	±0.00026	...	...
$a_{\rm Aa1-Aa2}$ (arcsec)	0.0005973	±0.0000089	...	...
$a_{\rm Wide}$ (AU)	2.501	±0.016	51.5	±5.6
$a_{\rm subsystem}$ (AU)	0.04166	±0.00032	1.81	±0.20
π (mas)	30.22	±0.26	...	...

Notes. Best-fit orbit parameters for the triple systems 63 Gem A and HR 2896. Quantities below the line were derived, and their uncertainties estimated using first-order error propagation.

planets of the solar system. Should other planetary systems also be preferentially coplanar, this suggests an important difference in the modes and timescales of planet versus binary formation.

6. DISCUSSION

6.1. 63 Gem A

With three luminous components, all of which can be studied spectroscopically, 63 Gem A is a valuable system for triple star studies. The short-period subsystem's very small separation (0.6 mas) would push the resolution limits of even long baseline interferometry. Because the contrast is low, a system operating at visible wavelengths (where spatial resolution is enhanced) and capable of precision closure phases (for imaging) could be used to continue studying this compelling system. The recently NSF funded Visible Imaging System for Interferometric Observations at NPOI (VISION) beam combiner will contribute to this effort.

6.2. HR 2896

The low-mass companion to HR 2896 is likely an M dwarf in either a nearly coplanar or anti-coplanar orbit to the wide binary itself. While a 0.2 $M_\odot$ white dwarf is also a possibility, this seems unlikely; such a low-mass white dwarf could only be produced by a low-mass star that would be unlikely to have evolved to that point by now, and almost certainly not before the more massive stars in the system would have evolved. With an anticipated separation of 19.5 mas, the M dwarf could easily be resolved by long baseline interferometry, though the high contrast will be challenging. An instrument operating at infrared wavelengths, where the contrast is lower, and capable of precision closure phases, such as MIRC at the CHARA Array, could be used for further study of this system.

PHASES benefits from the efforts of the PTI collaboration members who have each contributed to the development of an extremely reliable observational instrument. Without this outstanding engineering effort to produce a solid foundation, advanced phase-referencing techniques would not have been possible. We thank PTI's night assistant Kevin Rykoski for his efforts to maintain PTI in excellent condition and operating PTI in phase-referencing mode every week. Thanks are also extended to Ken Johnston and the U. S. Naval Observatory for their continued support of the USNO Double Star Program. Part of the work described in this paper was performed at the Jet Propulsion Laboratory under contract with the National Aeronautics and Space Administration. Interferometer data were obtained at the Palomar Observatory with the NASA Palomar Testbed Interferometer, supported by NASA contracts to the Jet Propulsion Laboratory. This publication makes use of data products from the Two Micron All Sky Survey, which is a joint project of the University of Massachusetts and the Infrared Processing and Analysis Center/California Institute of Technology, funded by the National Aeronautics and Space Administration and the National Science Foundation. This research has made use of the Simbad database, operated at CDS, Strasbourg, France. This research has made use of SAOImage DS9, developed by the Smithsonian Astrophysical Observatory. M.W.M. acknowledges support from the Townes Fellowship Program, Tennessee State University, and the state of Tennessee through its Centers of Excellence program. Some of the software used for analysis was developed as part of the *SIM* Double Blind Test with support from NASA contract NAS7-03001 (JPL 1336910). PHASES is funded in part by the California Institute of Technology, Astronomy Department, and by the National Aeronautics and Space Administration under Grant No. NNG05GJ58G issued through the Terrestrial Planet Finder Foundation Science Program. This work was supported in part by the National Science Foundation through grants AST 0300096, AST 0507590, and AST 0505366. M.K. is supported by the Foundation for Polish Science through a FOCUS grant and fellowship, by the Polish Ministry of Science and Higher Education through grant N203 3020 35.

Facilities: PO:PTI, TSU:AST, KPNO:CFT

REFERENCES

Abt, H. A., & Levy, S. G. 1976, ApJS, 30, 273
Colavita, M. M., et al. 1999, ApJ, 510, 505
Cumming, A., Butler, R. P., Marcy, G. W., Vogt, S. S., Wright, J. T., & Fischer, D. A. 2008, PASP, 120, 531

Cumming, A., Marcy, G. W., & Butler, R. P. 1999, ApJ, 526, 890
Eaton, J. A., & Williamson, M. H. 2007, PASP, 119, 886
Fabrycky, D., & Tremaine, S. 2007, ApJ, 669, 1298
Hartkopf, W. I., Mason, B. D., & Worley, C. E. 2001, http://www.usno.navy.mil/USNO/astrometry/optical-IR-prod/wds/orb6
Holman, M. J., & Wiegert, P. A. 1999, AJ, 117, 621
Kozai, Y. 1962, AJ, 67, 591
Lane, B. F., & Muterspaugh, M. W. 2004, ApJ, 601, 1129
Maedler, J. H. 1844, Dorpat Obs., 11, 3
Mason, B. D., Wycoff, G. L., Hartkopf, W. I., Douglass, G. G., & Worley, C. E. 2001, AJ, 122, 3466
Mason, B. D., Wycoff, G. L., Hartkopf, W. I., Douglass, G. G., & Worley, C. E. 2010, http://www.usno.navy.mil/USNO/astrometry/optical-IR-prod/wds/WDS
McAlister, H. A., Hartkopf, W. I., Hendry, E. M., Campbell, B. G., & Fekel, F. C. 1983, ApJS, 51, 309
Monnier, J. D., Berger, J.-P., Millan-Gabet, R., & Ten Brummelaar, T. A. 2004, Proc. SPIE, 5491, 1370
Muterspaugh, M. W., Lane, B. F., Kulkarni, S. R., Burke, B. F., Colavita, M. M., & Shao, M. 2006, ApJ, 653, 1469
Muterspaugh, M. W., Lane, B. F., Kulkarni, S. R., Konacki, M., Burke, B. F., Colavita, M. M., & Shao, M. 2010a, AJ, 140, 1631 (Paper III)
Muterspaugh, M. W., et al. 2010b, AJ, 140, 1623 (Paper II)
Muterspaugh, M. W., et al. 2010c, AJ, 140, 1657 (Paper V)
Muterspaugh, M. W., et al. 2010d, AJ, 140, 1579 (Paper I)
Sterzik, M. F., & Tokovinin, A. A. 2002, A&A, 384, 1030
Struve, O. 1878, Pulkova Obs., 9
ten Brummelaar, T. A., et al. 2005, ApJ, 628, 453